Transportation Research Part D 114 (2023) 103545

Contents lists available at ScienceDirect

Transportation Research Part D

journal homepage: www.elsevier.com/locate/trd

Estimation of electric vehicle battery capacity requirements based on synthetic cycles

Maite Etxandi-Santolaya [a,*], Lluc Canals Casals [b], Cristina Corchero [a]

[a] Catalonia Institute for Energy Research (IREC), Energy Systems Analytics Group, Jardins de les Dones de Negre 1, 2, 08930 Sant Adrià de Besòs, Barcelona, Spain

[b] Department of Engineering Projects and Construction, Universitat Politècnica de Catalunya-UPC, Jordi Girona 31, 08034 Barcelona, Spain

ARTICLE INFO

Keywords:
Driving cycle model
Electric vehicles
End of Life
Battery degradation

ABSTRACT

The adoption of the Electric Vehicle requires a switch towards a circular system to reduce their environmental impact. Under this framework, the correct sizing of the batteries and avoiding their underuse are key actions. Based on the analysis of real data, this work proposes a model to synthesize current profiles representative of trips containing urban and highway sections. The model is used to generate cycles for common daily driving distances. Different sized batteries are analysed at their beginning and end of life to evaluate their ability to provide the required range. Based on the results, it is suggested that the ongoing trend of battery capacity increase is not justified. The commonly assumed threshold of 70–80% State of Health has proved to be too conservative in most cases, allowing for an extension of the first life that should be individually defined based on functional aspects.

1. Introduction

Policymakers around the world have started to build a strong regulatory framework to support the adoption of the Electric Vehicle (EV), aiming to reduce the carbon emissions of the transportation sector (IEA, 2021). The sales of passenger EVs are expected to increase sharply, going from 3.1 million in 2020 to 14 million in 2025 (BloombergNEF, 2021).

This rapid growth has raised concerns regarding the sustainability of EVs, especially around the material requirements for battery manufacturing (Simon et al., 2015), which accounts for an important share of the environmental impact of the EV (Bauer et al., 2015).

The amount of metals needed to meet the demand for EV batteries, mainly for Lithium and Cobalt, is expected to surpass the known reserves by 2050 if low rates of recycling are maintained (Weil et al., 2018). Moreover, this prediction considers an average battery capacity of 25 kWh for full EVs. While this could be true for the early years of the electric mobility, when battery sizes of 16 and 24 kWh were common, current market trends suggest a constant increase in capacity (Kurdve et al., 2019). In fact, nowadays, the EV battery average capacity is around 50 kWh (UK Department for Transport, n.d.) and in the upcoming years, vehicles with capacities over 100 kWh are expected (Sanguesa et al., 2021).

The increase in battery capacity puts into question the suitability of the EV as a means to reduce the environmental impact of the transportation system. A recent life cycle assessment highlighted that the current trend of expanding the capacity is detrimental to

Abbreviations: BoL, Beginning of Life; BMS, Battery Management System; EoL, End of Life; EV, Electric Vehicle; PHEV, Plug-in Hybrid Electric Vehicle; SH, Semi-highway; SoC, State of Charge; SoH, State of Health; SU, Semi-urban; V2G, Vehicle to Grid.

* Corresponding author.
E-mail address: metxandi@irec.cat (M. Etxandi-Santolaya).

https://doi.org/10.1016/j.trd.2022.103545
Received 22 July 2022; Received in revised form 14 November 2022; Accepted 20 November 2022
Available online 30 November 2022

greenhouse gas impacts and can make battery EVs less competitive than other transport alternatives, like Plug-in Hybrid EVs (PHEV) or alternative fuel-based vehicles (Ellingsen et al., n.d.). Notice that in the referenced study the maximum battery size analysed was 60 kWh, which is still below many of the models found in the market nowadays.

It could be argued that the capacity increase is based on meeting the range requirements of the population. However, knowing that common trips in Europe rarely exceed 10 kWh (Canals Casals et al., 2019), most of the battery range of these new EV models may remain unused, which implies an inefficient use of materials.

In addition, due to the range reduction caused by degradation (Barré et al., 2013), batteries are considered to reach End of Life (EoL) for traction purposes once their State of Health (SoH) falls to 70–80 % (Martinez-Laserna et al., 2018). This means that regardless of the driving requirements or initial battery size, the same EoL threshold is applied to all batteries.

Several authors have started to question this threshold, arguing that, in most cases, lower values of SoH could be reached without affecting the EV performance (Canals Casals et al., 2019; Saxena et al., 2015). Other authors, however, suggest that the 70–80 % threshold could be too optimistic in some cases (Arrinda et al., 2021). It is therefore clear, that the EoL criteria for EV batteries should be revised to guarantee that the safety and performance requirements are met, while ensuring that the batteries do not experience an early retirement from the vehicle.

To consider the EV as the sustainable alternative for mobility, the EV framework requires a reconsideration of the current market trends and a shift towards a circular economy-based model (Richter, 2022). Although, large efforts are ongoing to improve the recycling processes (Sommerville et al., 2021) or to find new revenue streams, such as the use of retired EV batteries in second-life applications (Hua et al., 2021), these latest stages of a product lifetime for circularity value chains imply a higher use of resources and a lower value for circularity than those affecting the initial stages (Potting et al., 2018). Reducing material use (Nilsen, 2019) and extending the first life including sharing or additional services come as preferred options (Milios, 2021). These facts, applied to EV batteries, would mean either the production of smaller batteries, the redefinition of the EoL according to actual driving requirements or even the stacking of energy services beyond mobility.

The evaluation of the previous streams of circularity requires a solid understanding of the real-life driving requirements and the battery ageing pathways under different environmental conditions and driving patterns.

Battery degradation modelling and prognostics often rely on the use of standard driving cycles, both for analysis (Lawder et al., 2014) and for model validation (de Hoog et al., 2017) (Hosen et al., 2021). However, differences in ageing have been found between EVs subject to standard cycles and real-life ones (Baure and Dubarry, 2019).

In this sense, part of the research effort has been directed towards defining more realistic driving cycles (Ben-Marzouk et al., 2021; Zhao et al., 2020). These proposed cycles still hold an important limitation when applied to battery design and modelling, as they neglect the deviations in real-life driving patterns and their stochastic nature due to the use of a single cycle (Schwarzer and Ghorbani, 2013). Since car manufacturers often restrict access to real-life data, the generation of synthetic driving cycles can provide high value.

Synthetic driving cycles can be generated to account for the differences in behaviours of the population. The generated cycles can be used to evaluate the degradation caused by particular working conditions of the EV battery and analyse how the loss of performance can hinder the ability to meet the requirements at any point of a driving trip. This analysis is key to define how far the first life can go, to evaluate whether the battery is being used to its maximum potential and, if this is not the case, to promote sustainable practices to avoid inefficient battery use. Since the amount of data is not restricted, as it occurs when using data from real users, synthetic cycles can extend the analysis to cover more use cases.

The proposed models for the generation of synthetic driving cycles attempt to mimic real driving patterns. Driving cycles are represented by different profiles that show how variables like speed, acceleration, traction power or current in the battery evolve over time. Early work regarding driving modelling included a methodology to characterize a single driving cycle and obtain a synthetic one, with an arbitrary length (Tazelaar et al., 2009). The speed profile of the synthetic cycle is obtained based on the relationship between the previous speed values and the traffic circumstances, treated as random white noise, of the real driving cycle. Later, other authors proposed approaches based on finding the statistical distribution of key parameters of the speed and acceleration profiles of real driving (Schwarzer and Ghorbani, 2013) (Ravey et al., 2011). The generation of driving cycles has also been based on the Markov model and by using speed, acceleration and road slope as variables (Souffran et al., 2011). Another methodology to construct cycles, instead of using statistics-based methods, is based on chaining together segments of the original driving cycles. For this method, the real cycle is divided into so-called microtrips, which start and end in vehicle stops. Then, the synthetic cycles are built by selecting microtrips from the generated database (Quirama et al., 2021).

The existing models successfully generate synthetic speed profiles from real-life data. However, their application for battery performance assessment relies on the construction of an EV model to translate the speed into the current, which might be a major assumption. The different vehicle components must be modelled, along with the driver's commands to accelerate and brake. This additional work can be avoided by looking directly at the operation of the battery and the resulting profile to further model the current flows during the driving cycles.

This is, effectively, what recent studies are searching for: to obtain synthetic current profiles from direct battery information. However, most studies focus on charge profiles, such as (Schäuble et al., 2017), and, to the author's knowledge, only a couple have generated synthetic current profiles from real driving cycles. In one of these studies, two coupled feedforward Neural Networks were employed to model the charge and discharge profiles (Herle et al., 2021). The Markov Chain has also been used to generate synthetic current profiles, which uses transition probability matrixes to predict the current based on the previous state (Pyne et al., 2019). These approaches are a form of black-box modelling that output synthetic profiles but do not provide information on the key parameters of the drive cycle.

The methodology in this work is inspired by one of the probabilistic approaches reviewed that allows obtaining speed profiles

(Schwarzer and Ghorbani, 2013) but focusing on the current in the EV battery instead. In this work, the current profile of the battery during a driving cycle of the desired duration is stochastically generated based on the statistical description of key parameters obtained from real EV battery data. Therefore, the novelty of the proposed modelling consists of the direct analysis of the working conditions of the EV battery, avoiding the simplifications caused by using an EV model, and that provides a direct look into battery operation parameters instead of the black-box approach found in the literature.

The first part of the study aims to provide insight into the working conditions of the battery during real driving and to develop a driving cycle model that outputs realistic current profiles. The second part presents several applications of the model to analyse the requirements of different battery usages, both at the Beginning of Life (BoL) and at the EoL. The results allow discussing the adequacy of current battery capacities, evaluating whether the EoL threshold of 70–80 % is a good indicator of real driving needs, and reviewing how existing policies and market trends could be shifted towards more sustainable practices.

2. Methodology

The methodological framework for this study is provided in Fig. 1, which includes the main inputs, outputs and processes carried out.

The work starts by presenting an in-depth look at the operating conditions of the battery during driving, through the parametrization of the data collected from the Battery Management System (BMS) of real EVs (Sections 2.1 and 2.2). The outputs of these sections are probability functions, which are presented in Section 3.1, that represent how often each parameter occurs in real life. This analysis serves as the basis to construct the proposed driving cycle model and to generate synthetic current profiles (Section 2.3). The model is used to obtain the daily driving cycles for a year for several driver types, representative of the entire population, defined in Section 2.4, which are evaluated at two environmental conditions. The current profiles provide a picture of the actual capacity needs of the drivers. Differently sized batteries are analysed at their BoL and EoL, considering the fixed 80 % SoH threshold and a functional one, to evaluate whether they are able to provide the required driving range to each of the defined drivers (Section 3.3). The driving cycle model is validated in Section 3.2.

The input for this study (dataset 1 in Fig. 1) is the data collected from a real PHEV during 18 driving cycles in Barcelona, between April and November. The PHEV had a battery with a nominal capacity of 12 kWh and a nominal voltage of 320 V. For more details on the PHEV used and the trips performed, the reader is directed to the work by Canals et al. (Canals Casals et al., 2016a).

The use of a PHEV, instead of a full EV, avoids the differences in behaviour caused by range anxiety. Using a PHEV, the drivers are able to drive freely, without restricting high acceleration commands or high speeds, knowing that if the battery is depleted, they can switch to the combustion engine at any point. Therefore, the available data represents the natural driving patterns of the drivers. To eliminate the difference in the operation of the battery when used in hybrid mode, the trips have been selected to consider only the periods where the PHEV was driven in 100 % electric mode.

The available data from the BMS consists of the battery pack-related data (with its current, voltage, temperature and State of Charge (SoC)) and that of each cell in the pack (with its corresponding temperature and voltage profiles) at a frequency of 1 Hz.

Different drivers performed each of the available driving cycles, capturing a variety of driving styles and traffic conditions. The behaviour of the battery in different road types differs importantly and therefore, to be able to create a reliable model, it is necessary to group the input data based on the road type.

2.1. Classification of the real driving cycles

Even though the itinerary of each of the driving cycles is unknown, the energy consumption per unit of time provides an indicator of the road type. Based on values obtained from literature, the consumption per distance is assumed to be 0.176 kWh/km for urban driving and 0.189 kWh/km for highway driving, where high speeds increase consumption (Canals Casals et al., 2016b). These values can be translated to consumption per unit of time by considering that the average speeds for urban and highway driving are 31 km/h

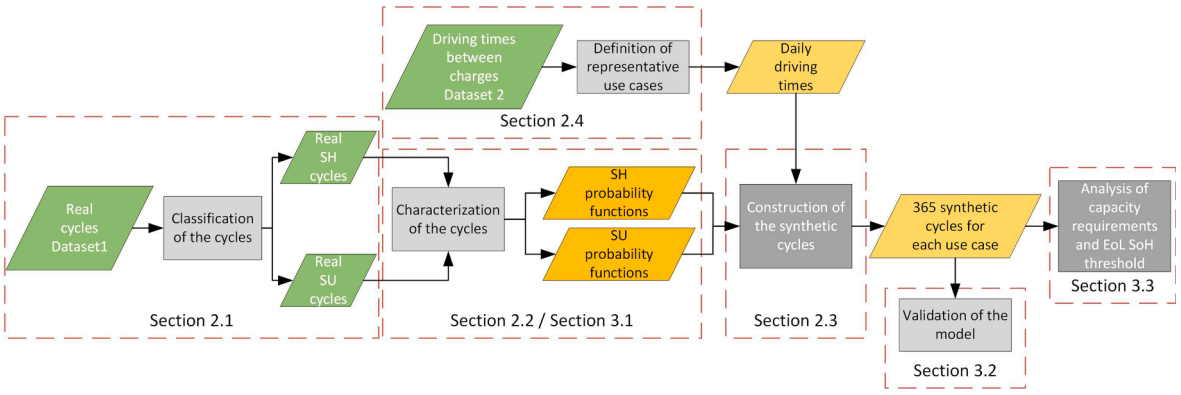

Fig. 1. Methodology framework of the study.

and 93 km/h respectively (André et al., 1994).

The reference consumption values are compared to the consumption of the real cycles. This last consumption is obtained from the power profile of the battery, which is calculated from the current and voltage profiles. Fig. 2 shows the consumption of each of the real driving cycles and the reference consumption for urban and highway driving. This representation allows observing that the real cycles are a combination of both road types, with a tendency towards highway sections in the cycles with higher consumption and urban in the lower consumption ones.

Therefore, the real cycles have been classified into two groups: semi-urban (SU) and semi-highway (SH), considering a threshold of 0.195 kWh/min, which is the middle value between the pure highway and pure urban driving. Therefore, SU cycles are representative of urban driving, with short highway sections and in SH cycles, highway driving is the dominant style. By analysing the driving cycles corresponding to each type, two models have been built: one for SU driving and the other for SH driving.

2.2. Characterization of the real driving cycles

In order to characterize both driving types in detail, each driving cycle is considered to contain a series of microtrips that take place until the final stop of the vehicle. Each of these microtrips is composed of discharge and regenerative braking periods, referred to as driving pulses, with an idle period in between them, where no current flows through the battery. Fig. 3 represents this way of conceptualizing the driving cycles.

For each period (discharge, regeneration, idle and final stop), representative parameters of the current profiles are extracted, and their statistical empirical distribution is built, considering 20 equally sized bins. The parameters considered and their description are presented in Table 1.

The first approach used relies on finding the cumulative probability function of each parameter. It can be shown by means of the appropriate parametric statistical tests that the existing data do not follow common distribution functions (e.g., gaussian, chi-square, etc.) and, therefore, empirical discrete probability functions are used. The usage of all available data for the definition of the probability functions preserves the stochastic nature of the input data.

2.3. Driving cycle generation procedure

The driving cycle models for SU and SH driving are built based on the previously described probability functions based on real data. The proposed model takes as input the trip duration and outputs the current profile with a resolution of 1 Hz.

The methodology to build the synthetic current profile is based on a stochastic simulation from the empiric probability functions. The sample for the parameters is obtained by generating a random seed that is used to extract the corresponding input value from each probability function.

The steps and inputs used to form the current profile are described below and represented in Fig. 4 following the reference nomenclature from Table 1.

1. Characterization of the idle periods: the first step is to find the number of idle periods that the trip will contain. Considering the desired duration of the driving cycle (d_{DC}), which is the input of the model, the frequency $I1$, obtained from the corresponding probability function, defines the number of idle periods (n) following Eq. (1).

$$n = I1 * d_{DC} \tag{1}$$

The duration of each idle period ($I_0 \cdots I_n$), is obtained from the probability function of $I2$. To avoid unrealistic driving trips, the total idle duration is not allowed to exceed 15 % and 19 % of d_{DC} for SU and SH respectively, which corresponds to the maximum percentages found in the real driving cycles. These idle periods are located symmetrically over the entire duration of the cycle, which defines the duration of the driving pulses (d_{DP}) in between the idle periods, as shown in Eq. (2).

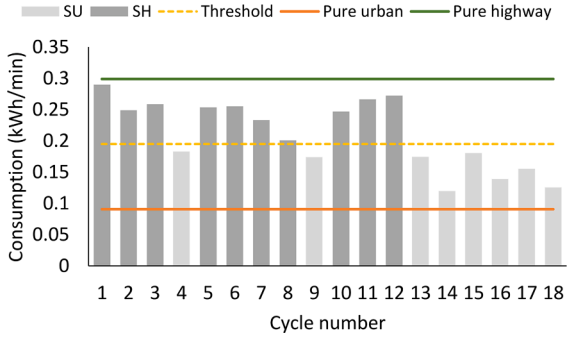

Fig. 2. Classification of SU and SH cycles based on the consumption.

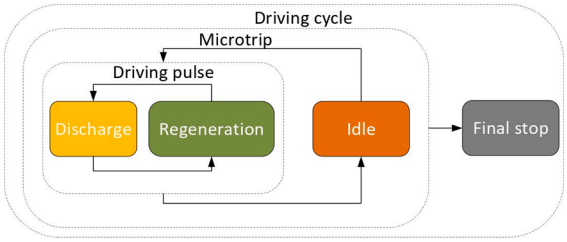

Fig. 3. Driving cycle schematic and nomenclature.

Table 1
Key parameters of the driving cycles and their description.

Ref	Name	Period	Description	Unit
I1	Idle frequency	Idle	Number of idle periods per minute	periods/min
I2	Idle duration	Idle	Duration of each idle period	s
I3	Before idle delta	Idle	Delta of current before an idle period	A
I4	After idle delta	Idle	Delta of current after an idle period	A
F1	Final stop delta	Final stop	Delta of current before the final stop	A
F2	Final stop delta rate	Final stop	Current delta rate of the final stop	A/s
D1	Discharge duration	Discharge	Duration of the discharge periods	s
D2	Discharge maximum current	Discharge	Maximum current reached in a discharge period	A
D3	Discharge delta current	Discharge	Average current delta during consecutive seconds during discharge	A
D4	Reduction after max discharge	Discharge	Reduction of the relative maximums after the maximum discharge current (D2) is reached	–
R1	Regen duration	Regeneration	Duration of the regen periods	s
R2	Regen maximum current	Regeneration	Maximum current reached in a regen period	A
R3	Regen delta current	Regeneration	Average current delta during consecutive seconds during regen	A
R4	Reduction after max regen	Regeneration	Reduction of the relative maximums after the maximum discharge current (R2) is reached	–

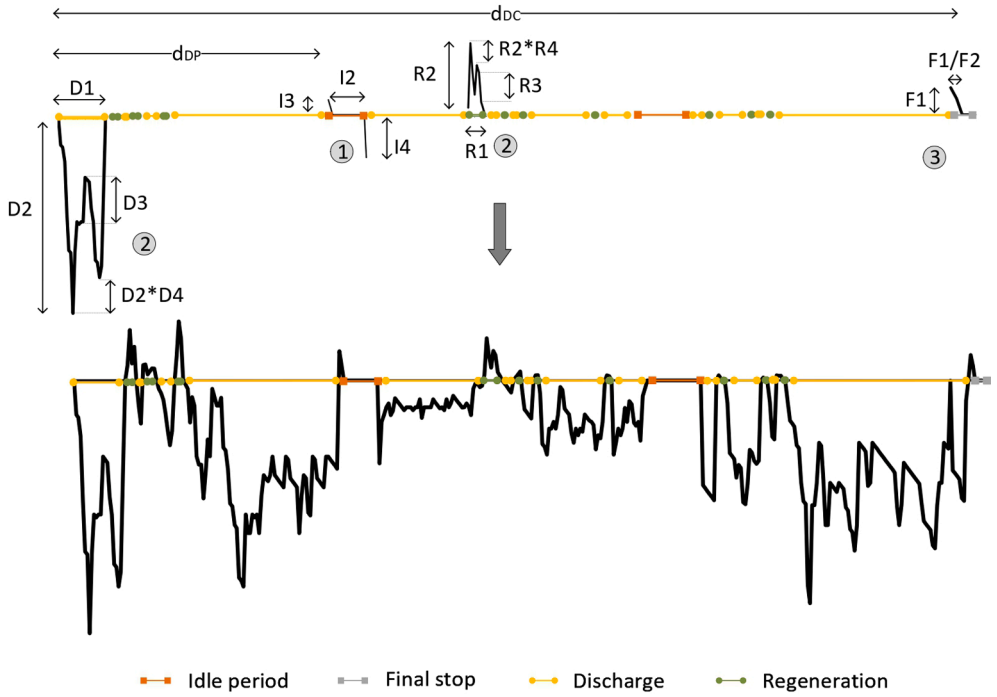

Fig. 4. Driving cycle generation procedure.

$$d_{DP} = \frac{1}{n}\left(d_{DC} - \sum_{i=0}^{n} I2_i\right) \quad (2)$$

The current during the entire idle period is set to zero, and the seconds immediately before and after the periods are characterized by the values extracted from the probability functions of $I3$ and $I4$. These values represent the jump in current that takes place before and after an idle period.

2. Characterization of the driving pulses: once the idle periods are defined, each period between them represents a driving pulse composed of consecutive discharge and regeneration periods. Each discharge or regeneration is defined by its duration, as extracted from the probability functions of $D1$ and $R1$, respectively.

The current for each second of these periods is calculated until the total duration is met. Based on the previous current value, the current of the following second is calculated by adding the delta current extracted from the probability functions of $D2$ or $R2$. At this step, additional conditions are imposed. Firstly, the maximum current is not allowed to be higher than the value extracted from the probability functions of $D3$ or $R3$. In addition, the maximum current is only allowed to be reached once during each regeneration or discharge period. The following relative maximums are reduced by the values extracted from the probability functions of $D4$ or $R4$. This process for calculating the current is performed until the duration of the drive pulse (d_{DP}) is reached.

3. Characterization of the final stop: the final part of the last drive pulse is overwritten with the current profile of the final stop, which defines how the battery reaches the end of the trip. This profile is characterized based on the values of the current delta ($F1$) and the rate ($F2$) and assuming a progressive decrease of the current until it reaches zero.

This process allows building the synthetic current profile for the desired trip duration and road type. For this study, an important parameter is the consumption of the trip. This value is obtained by considering the power profile calculated from the current profile and an average voltage on the battery, obtained by analysing the real operation of the PHEV in the input dataset 1.

2.4. Use case definition

The developed model is used to obtain the daily driving profiles of several drivers during an entire year to evaluate how different-sized batteries are able to meet the capacity requirements according to their SoH.

In order to define representative driving trips, data collected from 24 EVs over 1.5 years and 3 European regions have been considered (dataset 2 in Fig. 1). Two of the regions are representative of urban driving and one contains highway sections. Therefore, the data from the two urban regions have been grouped to represent SU driving and the other region has been considered for SH.

Based on the duration of the trips between charges, the values that cover 50 % and 90 % of the trips have been extracted. Using the driving cycle model and these durations, four driver types are defined and their daily synthetic driving cycles are generated for an entire year. These driver types represent users who have habits when using their EVs, like driving on SU or SH roads and covering specific distances. Instead of considering the same duration of driving for each day, to add a stochastic factor to the analysis, the daily driving time is obtained from a normal distribution where the mean is the duration presented in Table 2 and the standard deviation is 5 % of the mean. By using a normal distribution of the driving durations, the study focuses on relatively homogenous drivers, such as commuting ones. However, it should be highlighted, that in the analysis of the EoL requirements, the longest 5 % of the trips have been assumed to be covered by other means of transport, as will be further discussed in Section 4. This implies that the results also reflect drivers that sporadically perform long-distance trips but choose an alternative to the EV for those trips.

A critical aspect that limits the performance of EVs in several parts of the world is the environmental condition. Under cold temperatures, besides the effects related to battery degradation such as lithium plating (Jaguemont et al., 2016) or the internal resistance increase that reduces the useful capacity, the specific energy consumption of the EV can be substantially higher than in warmer climates. This is due to higher energy losses in the efficiency of the battery and for the auxiliary heating services of the vehicle.

Therefore, even with the same driving patterns and nominal capacity, the functionalities required by the driver can be compromised due to cold temperatures. To account for this climate dependency, for each of the driver types presented above, an additional use case is considered in which the consumption per trip is increased by a factor of 29 %, obtained from comparing the EV consumption at an average annual temperature of 18 °C and 8 °C (Al-Wreikat et al., 2022).

For each of the use cases, 6 differently sized batteries (16, 24, 30, 40, 60 and 90 kWh) representative of the current EVs on the road are analysed. Considering that the driving cycle model was developed for a 12 kWh PHEV, the consumption has been corrected to account for the differences in weight.

Fig. 5 shows the weight of EVs with different battery capacities. The weight of the PHEV used to build the driving model is marked in yellow, which serves as the reference to define the correction factors. Notice that the PHEV has additional components like the combustion engine and tank, which increase the weight compared to an EV with the same battery capacity. Considering average

Table 2
Definition of the driver types according to the road and average driving time.

Driver type	Road type	Trips covered	Average daily driving time (mins)
SU_{50}	SU	50 %	52
SU_{90}	SU	90 %	126
SH_{50}	SH	50 %	44
SH_{90}	SH	90 %	109

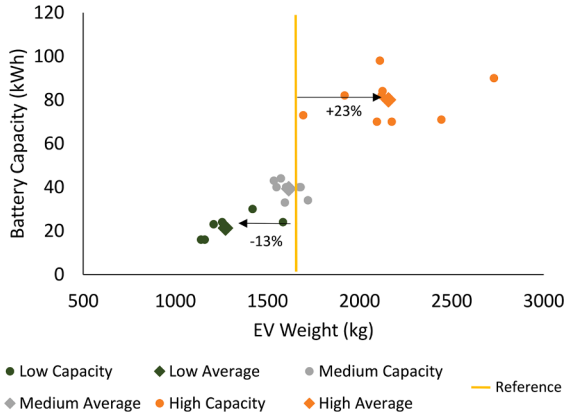

Fig. 5. EV Weight based on the battery capacity for different models.

weights, a reduction in the consumption of 13 % has been applied for low-capacity EVs (16 and 24 kWh) and an increase of 24 % for high-capacity ones (70 and 90 kWh). The average weight of the medium capacity EVs (30 and 40 kWh) is close to the reference value and therefore, no adjustment has been applied for these cases. To check the accuracy of the correction factors obtained using the EV weight, a WLTP consumption-based analysis was performed, which yielded similar results.

Therefore, a total number of 48 use cases (battery-driver-climate combinations) are analysed at Beginning of Life (BoL) and EoL.

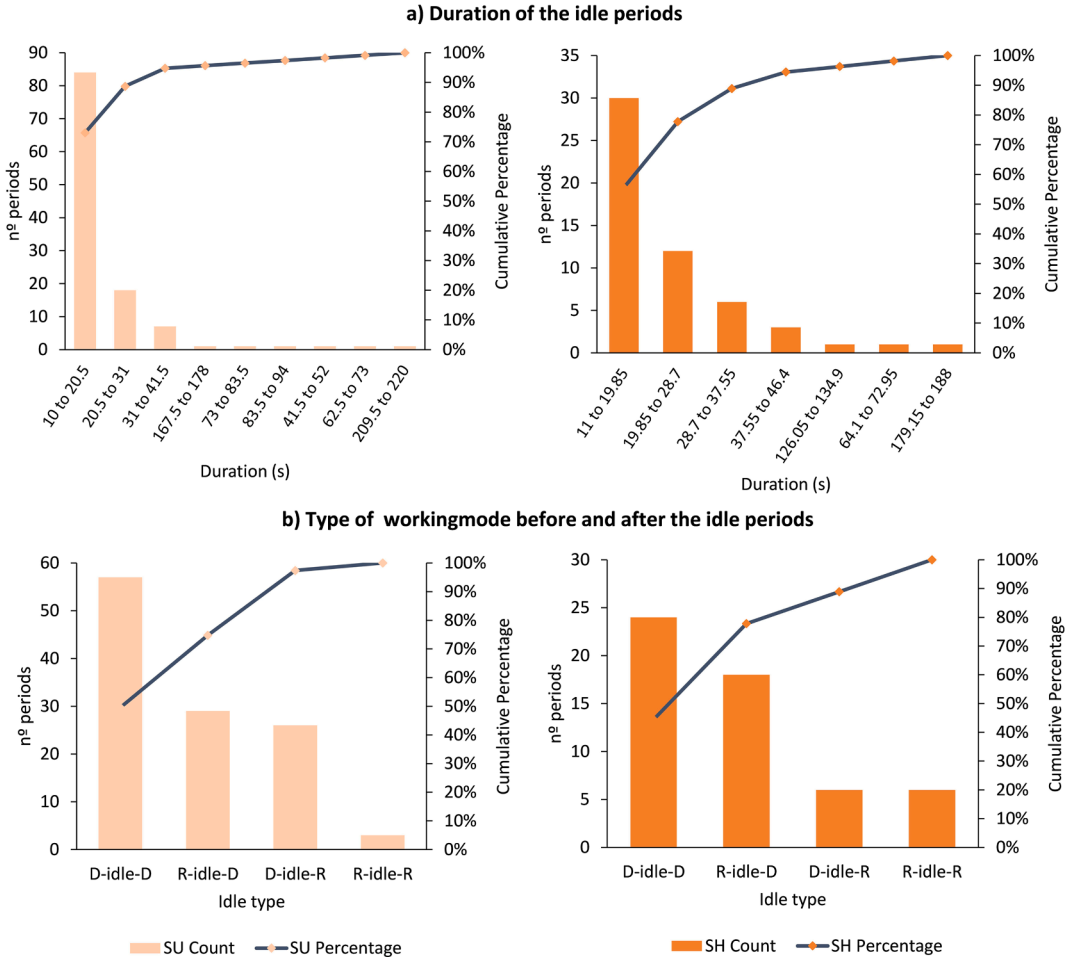

Fig. 6. Idle period distributions.

The EoL is calculated in two ways: 1) using the fixed threshold of 80 % SoH and 2) using a functional one that allows providing the energy required by 95 % of the trips, without falling below 60 % where other aspects should be addressed (Etxandi-Santolaya et al., 2022).

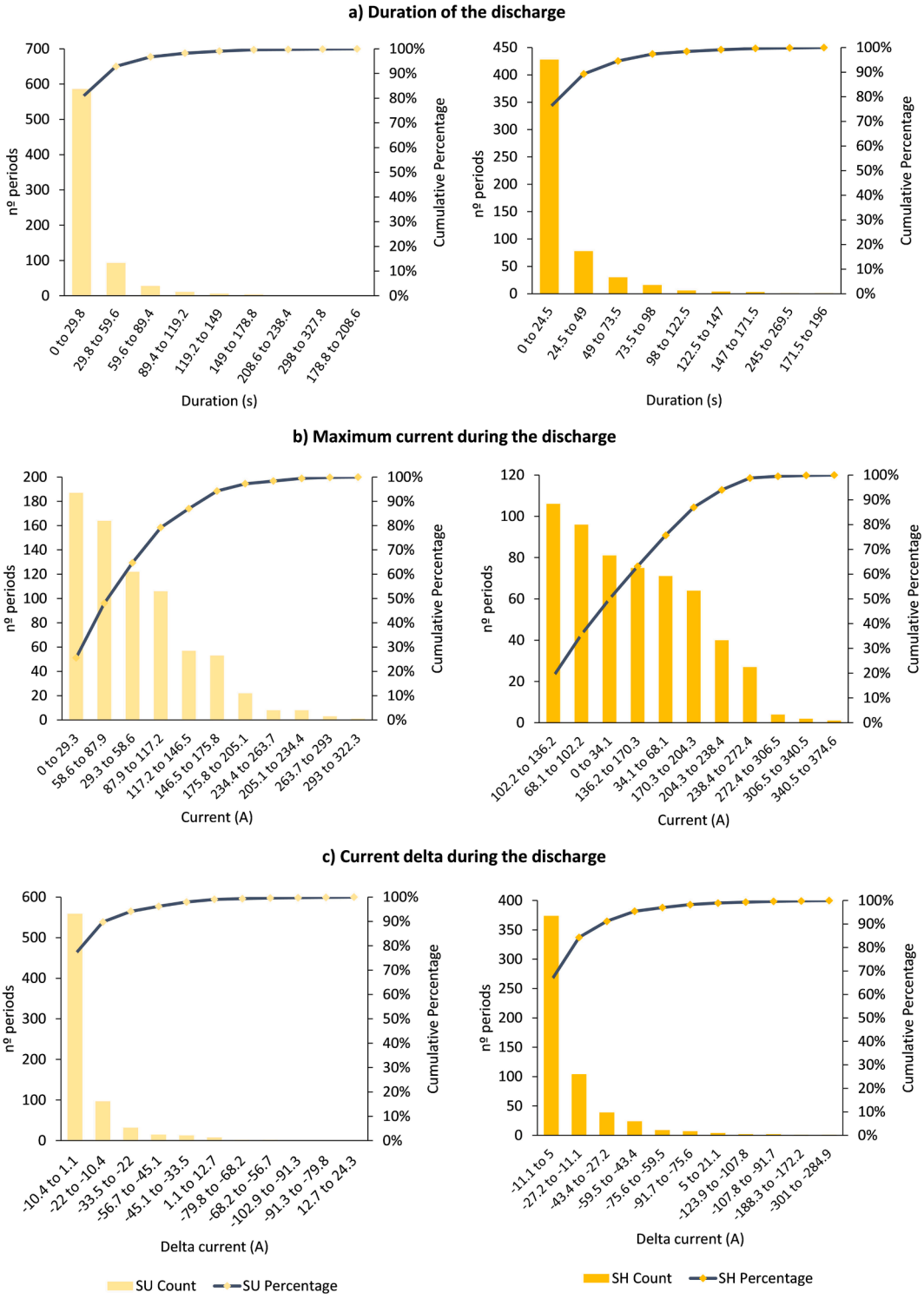

Fig. 7. Discharge period distributions.

3. Results

3.1. Real driving cycle parameters

First, the driving cycle parameters of the real data are presented. Due to the large number of distributions, only the most relevant

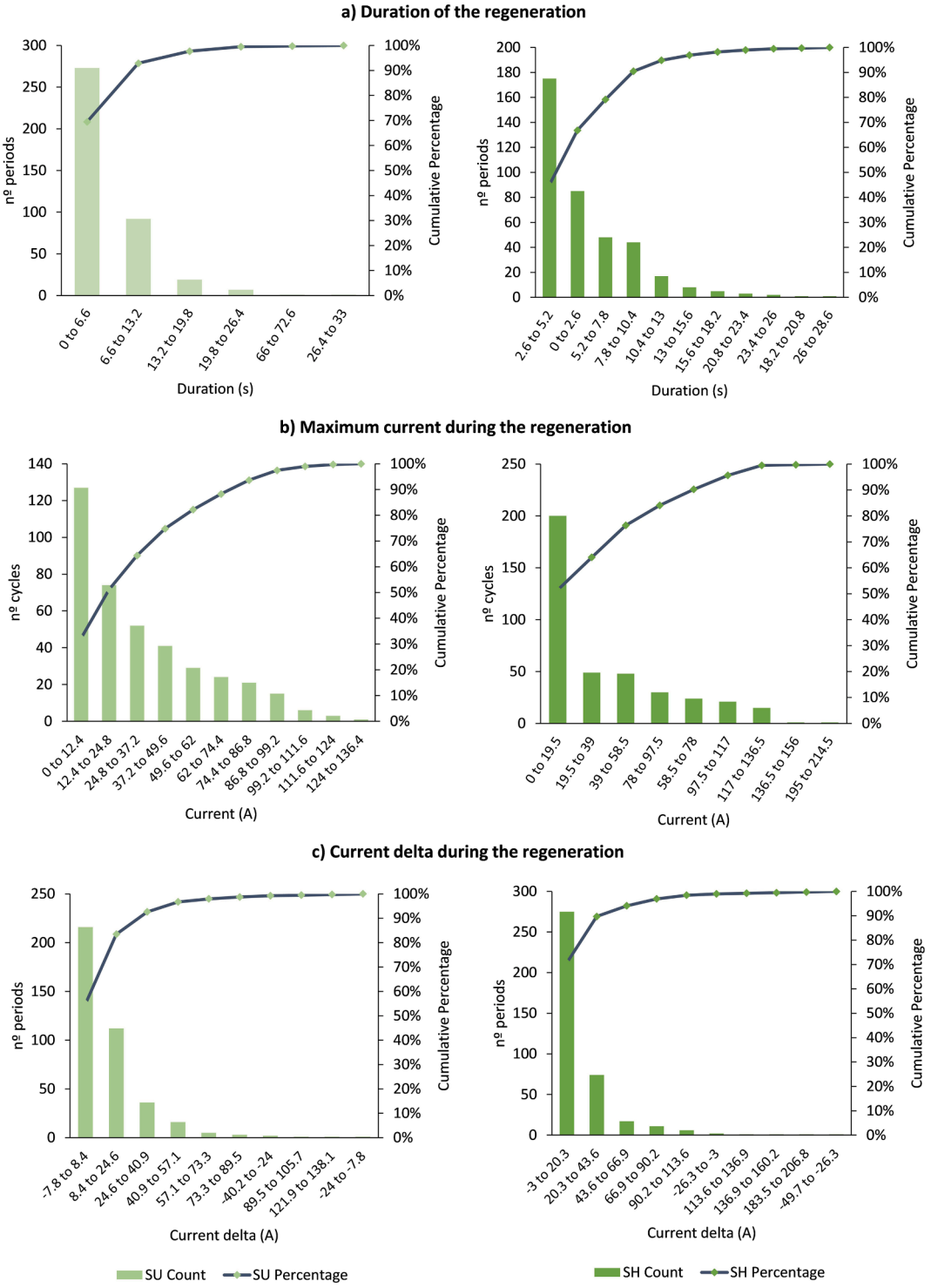

Fig. 8. Regeneration period distributions.

ones are plotted, with a reduction of the number of bins for ease of representation in several cases. In the histograms, the left side represents SU and the right side SH. The entire probability functions of all parameters are provided as supplementary material, which the reader can access for a more in-depth analysis.

3.1.1. Idle periods

The duration of the idle periods ranges between 10 and 220 s and 10–188 s for SU and SH driving, respectively. Fig. 6a shows how for both road types, the most frequent stops last less than 20 s.

For both SU and SH, during the seconds before and after an idle period, the battery often recorded discharge currents, which suggests that in many cases the EVs were not able to recover energy through regeneration, even if the car was braking to arrive at the idle period. This is shown in Fig. 6b which classifies the idle periods depending on whether the battery charged through regeneration (R) or discharged (D) before and after the period.

On average, the SU EVs remain between 5 and 17 % of the time in idle mode (11 % on average) and their frequency of the stops is between 0.19 and 0.40 stops/min (0.31 stops/min on average). For SH cycles, the percentage of idle time over the total is reduced to 2–15 % (7.5 % on average), validating the assumption that these cycles contain lower urban sections and more highway ones. The frequency of the stops, in this case, is 0.04–0.41 stops/min (0.18 stops/min on average).

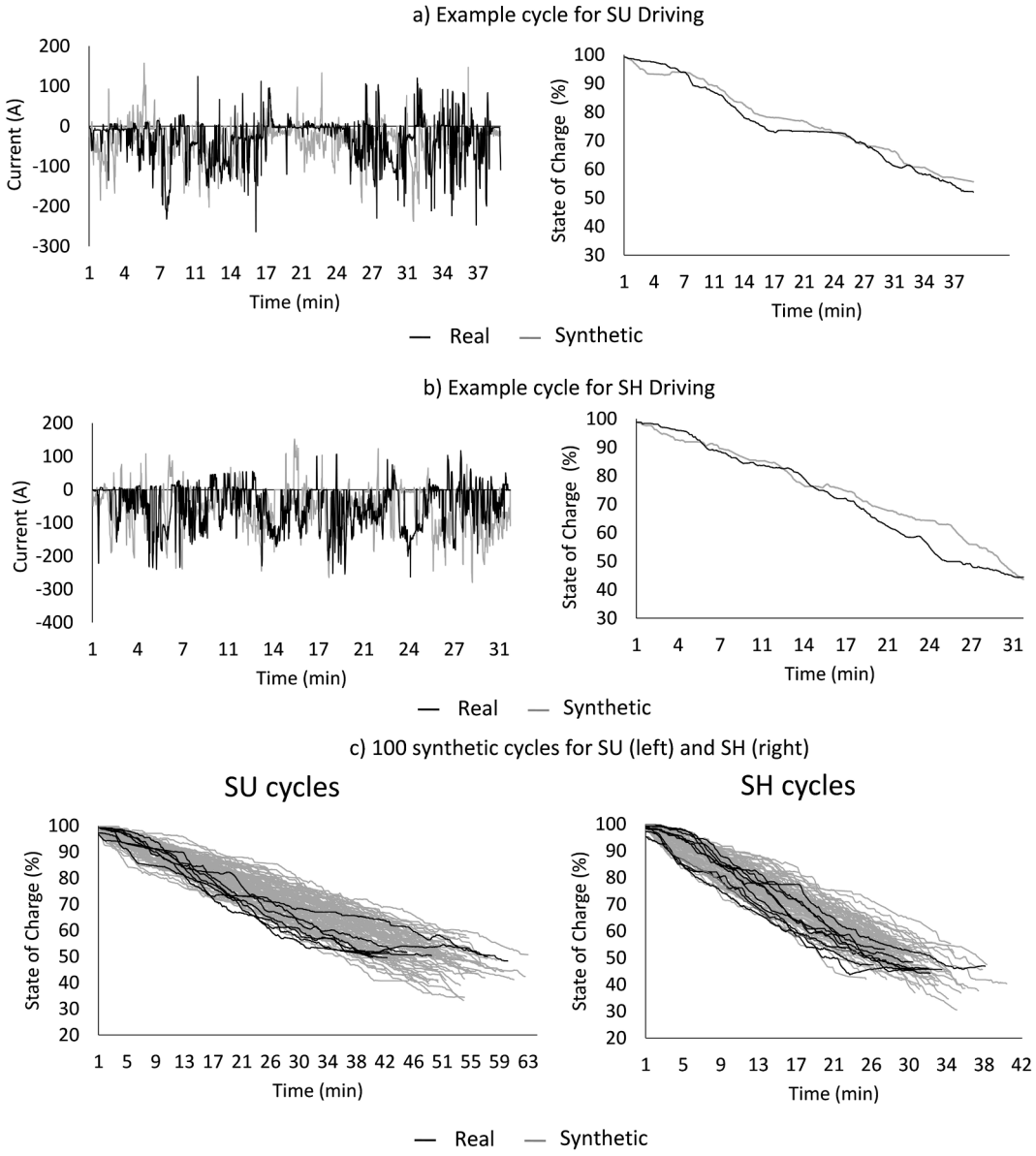

Fig. 9. Synthetic drive cycles compared to the real ones.

3.1.2. Discharge periods

Fig. 7 shows the main distributions obtained for the discharge periods for SU (left) and SH (right) driving. The distributions of the duration of these discharge periods are shown in Fig. 7a. SU driving shows a tendency towards shorter discharges, unlike SH where the most frequent discharge duration is around 2 min, most likely due to its highway driving nature.

Fig. 7b shows the distribution of the maximum current during discharge. Notice how the maximum currents tend to be higher for SH driving than for SU driving.

The change in the discharge current, from second to second, is in most cases below 10 A, however, spikes of 100 A have been recorded, which could take place during a sudden acceleration or increase of road grade while driving. The distributions of the discharge current delta values are shown in Fig. 7c, where positive values represent a decrease in the current and negative values represent increases.

3.1.3. Regeneration periods

Fig. 8 shows the main distributions obtained for the regeneration periods for SU (left) and SH (right) driving. Even if longer durations are occasionally recorded, the most common regeneration periods last only a few seconds (less than 7 s for the majority of cases), as shown in Fig. 8a.

The maximum regeneration currents are shown in Fig. 8b. In this case, the differences between SH and SU driving are not substantial, suggesting that the regeneration may be limited by the battery itself.

Fig. 8c shows the change in the current during regeneration in a timespan of a second. Although spikes in the regeneration current of higher than 100 A have been recorded, the regeneration current often changes more slowly, with usual current deltas of below 8 A for SU and 20 A for SH. In the figure, positive values correspond to an increase in the current and negative ones to a decrease.

3.1.4. Final stops

Similarly to the idle periods, for the idle periods, the current before the stop is between 1 and 8 A. In this case, none of the cycles analysed allowed for regeneration before the final stop, and all presented discharge currents. Similarly, to the moments before the idle periods, the EVs were not able to recover energy through regeneration before the final stop. This can be caused by the low speeds at which the EV drives when parking.

3.2. Driving cycle model validation

Fig. 9a and Fig. 9b show one synthetically generated cycle for SU and SH, respectively, compared to a real one with the same duration. The current profile is shown on the left and the SoC profile on the right. The synthetic current profiles show a good similarity with the real ones and the maximum currents are in the same order of magnitude for both charge and discharge.

Fig. 9c shows the SoC profiles of 100 synthetic cycles for SU (left) and SH (right). It is worth mentioning that the real profiles show different behaviours depending on the trip period. The real SoC profiles show that the highest energy consumption takes place during the middle part of the trip, once the EV is on the road. For the trip start and end, where the vehicle may be getting in or out of the parking, the SoC profiles show a flatter shape. The synthetic profiles show that the model can generate cycles capturing the average usage pattern throughout the entire trip.

To validate the developed model, the annual driving cycles generated for the 4 driver types (Table 2) are compared with the real data. Table 3 shows the average consumption for the synthetic cycles compared with the one from the real cycles. The average consumption from the real cycles is obtained by finding the average consumption of all the cycles corresponding to each road type.

3.3. Evaluation of the capacity requirements

The plots from Fig. 10 represent the BoL batteries of different sizes, including, in green the average energy consumption for each use case, in yellow the maximum one and the remaining in grey the unused available capacity. If a battery cannot provide the required range at BoL, it is marked in red. In addition, the EoL capacity is marked by a red marker for the fixed SoH threshold and a black one for the functional one that covers 95 % of the driving trips. The first thing analysed is the minimum-sized battery required to fulfil all the driving trips at BoL.

- SU_{50} is covered by the 16 kWh battery for regular and cold climates.
- SU_{90} requires a 30 kWh for the regular climate, which is not enough in a cold climate where a 40 kWh battery is needed.
- SH_{50} is covered with a 16 kWh battery for regular climates and a 24 kWh one in cold climates.

Table 3
Average consumption of the synthetic cycles vs real ones.

Driver Type	Average Synthetic (kWh/min)	Average Real (kWh/min)	Rel Error
SU_{50}	0.152	0.158	−3.68 %
SU_{90}	0.151		−3.89 %
SH_{50}	0.254	0.255	−0.37 %
SU_{90}	0.253		−0.68 %

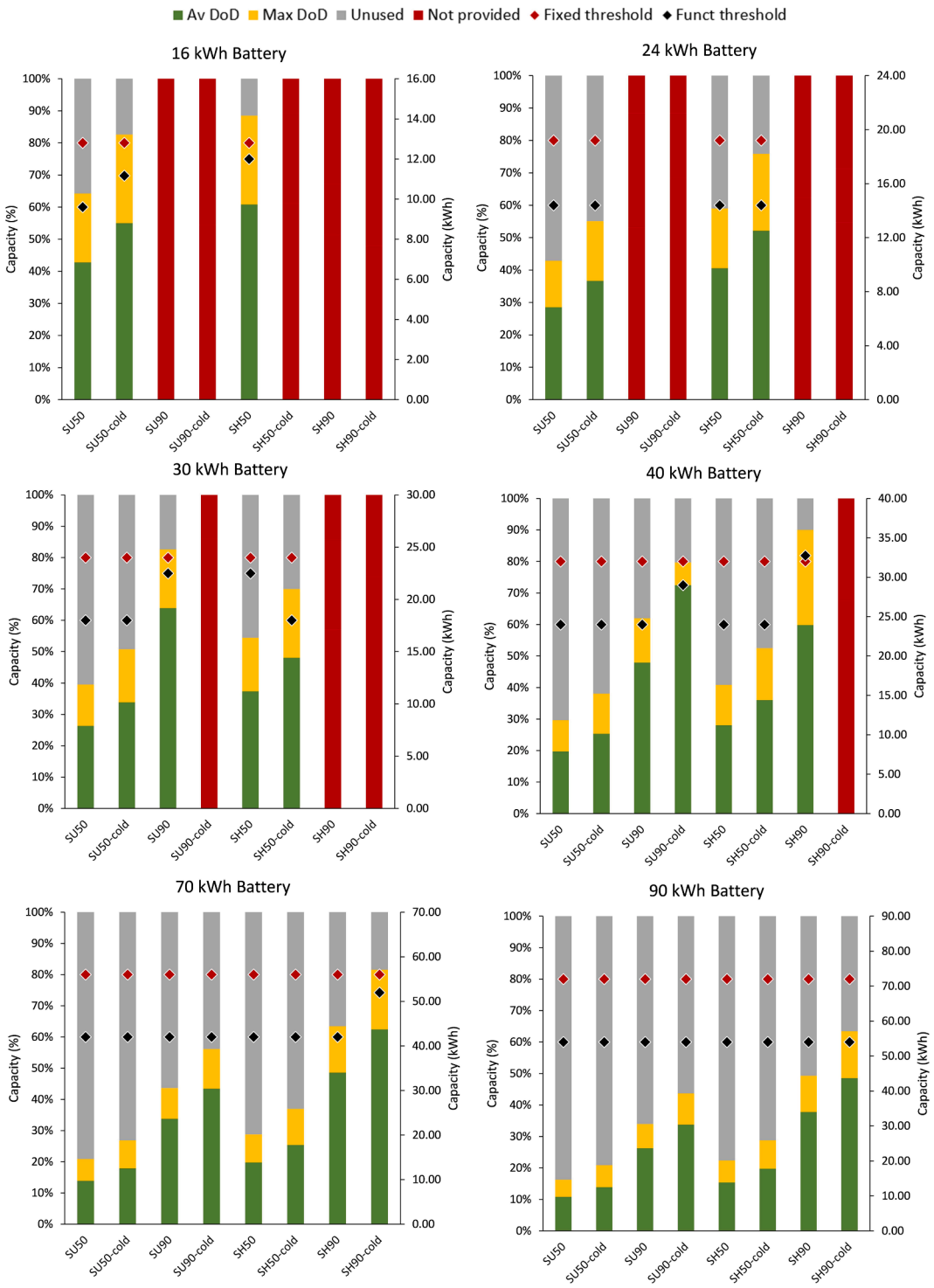

Fig. 10. Minimum and average DoDs and EoL SoH values.

- SH_{90} is the most demanding case for which a 40 kWh battery is required for the regular climate and a 70 kWh one under cold climate.

If the battery is not the minimum-sized one, the unused capacity is substantial, especially for SU driving. For the case covering 50 % of the population, choosing a battery over 24 kWh implies not using over half of the available capacity at BoL. For the 90 % case, this

happens around 70 kWh. SH driving is more demanding, as its consumption per unit time is higher. For the 50 % case, batteries over 40 kWh are severely underused. For the 90 % SH use case, batteries of 90 kWh and above are not used to their potential, as the average driving trip consumes only 50 % of the battery at BoL.

Regarding the cases covering 50 % of the population, even for the 16 kWh battery, the EoL can be postponed below 80 % SoH without creating any limitations in range. The only exception happens for the SH_{50} case in a cold environment, as the functional EoL is located at 81.9 %, above the fixed one. For 90 % of the population, the EoL can also be postponed for large batteries of 70 or 90 kWh even in cold climates.

Fig. 11 shows the difference between the fixed and functional thresholds used in this study. Highlighted in red appear the cases where the BoL battery cannot provide the required range, in green the cases where the EoL can be extended below the fixed SoH threshold and in orange the case for which the EoL is reached before 80 % SoH. Most cases allow a reduction of 20 %, corresponding to the EoL SoH of 60 % chosen for safety purposes. For the other cases where the EoL is found below the 80 % threshold, the first life can be maintained for an additional 5–10 % decrease of the SoH.

Based on an improvement to a degradation model developed using real-world EV data, which allows estimating the degradation of the EV battery depending on its age (Bibiloni-Mulet, 2020), the extension of the EoL has been translated to years. The additional life that a battery could have in the EV goes from 1.4 to 8.9 years for high-capacity batteries.

4. Discussion

Results highlight two important aspects regarding the current trends in the EV market. First, there is little evidence to support the need for a constant increase in battery capacity. As discussed in the introduction, current EV models sold on the market have on average 50 kWh. However, the 24 kWh battery has shown to be sufficient (even postponing the EoL) to cover the capacity needs of 50 % of the population. The 30 or 40 kWh batteries are sufficient to cover 90 % of the population driving on SU roads, and the 70 kWh one for SH. Therefore, batteries with capacities over 70 kWh remain severely underused for the majority of the cases. The underuse of EV batteries does not help to minimize the environmental impact of the transportation sector, which was the largest motivation for switching to electric-based mobility in the first place (Leurent and Windisch, 2011).

Secondly, for those cases where the battery at BoL can cover the daily mileage, the EoL threshold has proven to be too restrictive. Only in one of the cases studied (SH_{90} with 40 kWh) the 80 % threshold was too low. For the rest of the cases, the EV first life could last longer than expected with the 70–80 % SoH threshold.

This is something to be studied individually for each EV, by developing a methodology to define a functional EoL based on the battery size, environmental conditions and driving pattern. Future lines of research of the authors will deal with finding the EoL that is tailored to each driver and provides information on when and with which SoH the EV battery will actually be retired. In most cases, the functional EoL has not been defined by a lack of available capacity, but because the SoH arrived at 60 %. At this point, other aspects must be studied, like entering the ageing knee or the increase of the internal resistance that can generate underperformance or safety-related issues. Further work will be required to evaluate whether these aspects might force an early retirement of the battery before capacity constraints appear.

This study has shown how the manufacturing of lower-capacity batteries could be promoted while not compromising drivers' satisfaction. It should be highlighted that the study has been centred towards users with relatively homogenous trips. For those users that would occasionally perform longer trips, rather than oversizing the EV battery, which would remain underused most of the time and generate a larger environmental impact (Marmiroli et al., 2020), other alternatives should be considered. The first option could be choosing other means of transport for that trip, including public transportation or renting an internal combustion engine vehicle. The second option, which is also aligned with a big part of the research effort and investments, is to promote fast charging. With the deployment of adequate technology and infrastructure, fast charging could enable smaller batteries to cover longer distances by adding an intermediate charge in the trip (Hu, 2019).

The shift of the manufacturing trends towards lower capacities is in line with the environmental targets that aim to reduce the carbon footprint of the transportation sector and provides a solution to face the potential shortage of materials in the upcoming years. However, this alternative is not considered when looking at current policies. The New EU regulatory framework for batteries, proposed in December 2020, acknowledges the need to promote a circular economy-based treatment of the batteries. In particular, battery reuse and recycling are considered key pillars to reduce raw material extraction and maintain the value of the materials for longer (European Commission, 2020), leaving aside the non-use of resources in the first place.

As highlighted by policies and research efforts, recycling is the only way to decouple the production of batteries from the available raw materials. Nevertheless, recycling processes still face many limitations, such as a lack of sufficient investment and the need for higher economies of scale to be profitable against raw material extraction (Beaudet et al., 2020). Until a closed-loop system is achieved, reducing the battery capacity can provide a powerful tool to reduce stress on raw material extraction.

Regarding reuse, battery second-life applications provide a way to extend the useful life of the EV battery once retired from the vehicle by making use of its residual value, which is an action supported by the circular economy. These applications are being funded by many European research projects and are being deployed by several start-ups. However, second-life applications still face economic and technical uncertainties (Martinez-Laserna et al., 2018). In fact, as this study has shown, the expected SoH value of retired batteries is likely to be lower than the 70–80 % SoH assumed in second-life assessments. Starting the second life with higher levels of degradation may compromise the technical viability of the second life and reduce the economic profit (Montes et al., 2022). However, these effects may be in fact positive considering that second-life markets are expected to be saturated in the upcoming years (Kotak et al., 2021). Considering the market saturation, reducing the battery capacity would also avoid sending to recycling batteries with residual

	SU50	SU50 cold	SU90	SU90 cold	SH50	SH50 cold	SH90	SH90 cold
16 kWh	-20.0%	-10.2%			-5.0%			
24 kWh	-20.0%	-20.0%			-20.0%	-20.0%		
30 kWh	-20.0%	-20.0%	-5.0%		-5.0%	-20.0%		
40 kWh	-20.0%	-20.0%	-20.0%	-7.5%	-20.0%	-20.0%	1.9%	
70 kWh	-20.0%	-20.0%	-20.0%	-20.0%	-20.0%	-20.0%	-20.0%	-5.8%
90 kWh	-20.0%	-20.0%	-20.0%	-20.0%	-20.0%	-20.0%	-20.0%	-20.0%

Fig. 11. Functional EoL compared with the fixed threshold.

value.

A high battery capacity, however, provides an important marketing tool and for this reason, it is unlikely that manufacturers will reduce the ranges of EVs in the short term, unless forced to by legislation or lack of available material. As discussed in a recent study, if the same market trends are maintained, a large number of high capacity batteries will reach the EV EoL in a healthy state (Casals et al., 2022). In that case, to avoid the underuse, other sources of circularity should gain more weight, such as stacking other services during the battery first life, namely through Vehicle to Grid (V2G) services. In this study, large batteries have shown to have sufficient capacity to provide these services, while not compromising the daily driving requirements. V2G can allow exploiting the first life of batteries that would otherwise remain underused, while providing an important contribution to the grid and generating revenue for the owners (Ma et al., 2012). Prioritizing V2G over reuse is supported by the previously mentioned limitations of the second-life applications and by the circular economy guidelines, which promote actions with the least resource leakage. The deployment of V2G only needs a bidirectional charger, in front of the refurbishing, transportation and additional components that second-life batteries require.

5. Conclusions

This study has provided a close look into the operation of EV batteries during real-world driving, which allows understanding the conditions that batteries are subject to during their first life. The available driving cycles have been divided into idle, regeneration, discharge and final stop periods, identifying key parameters in each case. Based on these parameters, a driving cycle model has been built for two road types containing a different share of urban and highway sections. Even though the dataset was limited, it captured the different driving styles of several users. The methodology followed can be replicated by researchers with access to a higher number of observations and allows obtaining synthetic current profiles representative of real driving.

Based on the developed model, this work has synthesized several current profiles performed by different drivers to evaluate the ability to meet the capacity requirements at BoL and EoL. 50 % of the usual urban and highway driving can be covered with a 16 or 24 kWh battery, depending on the climate. For other drivers, batteries over 30 or 40 kWh are needed to cover the required range. In the most extreme case, corresponding to highway driving for almost 2 h in a cold climate, the minimum sized battery was 70 kWh. However, these cases are not the most representative of the population, and therefore most driving use cases can be covered with smaller batteries than those currently appearing on the market.

Shifting market trends towards lower battery capacities has the potential to decrease the carbon footprint and reduce the need for raw material extraction, which are pressing issues that affect the sustainability of the EV. If large batteries are maintained, sustainability premises ask for additional use of the battery through V2G services to exploit their first life as much as possible.

The study also shows how current battery sizes can provide the required range even at lower SoH than the commonly assumed 80 % EoL threshold. Only in one of the analysed cases, the functional EoL was found to be at a higher SoH value than 80 %. This means that, generally, batteries are assumed to be retired too early from the EV and, therefore, if a new EoL is defined for each case, the duration of their first life and the SoH at the retirement point could be more accurately predicted, which would substantially affect the assessment of second-life applications.

Author contributions

All authors have read and agreed to the published version of the manuscript.

Funding

This project has received funding from the European Union's Horizon 2020 research and innovation program under grant agreement No. 963580. This funding includes funds to support research work and open-access publications.

CRediT authorship contribution statement

Maite Etxandi-Santolaya: Conceptualization, Data curation, Formal analysis, Methodology, Software, Validation, Visualization, Writing – original draft, Writing – review & editing. **Lluc Canals Casals:** Conceptualization, Funding acquisition, Project

administration, Resources, Supervision, Validation, Writing – review & editing. **Cristina Corchero:** Funding acquisition, Project administration, Resources, Supervision, Validation.

Declaration of Competing Interest

The authors declare that they have no known competing financial interests or personal relationships that could have appeared to influence the work reported in this paper.

Acknowledgement

Lluc Canals Casals is a Serra Hunter Fellow.

Appendix A. Supplementary data

Supplementary data to this article can be found online at https://doi.org/10.1016/j.trd.2022.103545.

References

Al-Wreikat, Y., Serrano, C., Sodré, J.R., 2022. Effects of ambient temperature and trip characteristics on the energy consumption of an electric vehicle. Energy 238, 122028. https://doi.org/10.1016/j.energy.2021.122028.

André, M., Joumard, R., Hickman, A.J., Hassel, D., 1994. Actual car use and operating conditions as emission parameters: derived urban driving cycles. Sci. Total Environ. 146–147, 225–233. https://doi.org/10.1016/0048-9697(94)90241-0.

Arrinda, M., Oyarbide, M., Macicior, H., Muxika, E., Popp, H., Jahn, M., Ganev, B., Cendoya, I., 2021. Application Dependent End-of-Life Threshold Definition Methodology for Batteries in Electric Vehicles. Batteries 7, 12. https://doi.org/10.3390/batteries7010012.

Barré, A., Deguilhem, B., Grolleau, S., Gérard, M., Suard, F., Riu, D., 2013. A review on lithium-ion battery ageing mechanisms and estimations for automotive applications. J. Power Sources 241, 680–689. https://doi.org/10.1016/j.jpowsour.2013.05.040.

Bauer, C., Hofer, J., Althaus, H.-J., Del Duce, A., Simons, A., 2015. The environmental performance of current and future passenger vehicles: Life cycle assessment based on a novel scenario analysis framework. Appl. Energy 157, 871–883. https://doi.org/10.1016/j.apenergy.2015.01.019.

Baure, G., Dubarry, M., 2019. Synthetic vs. Real Driving Cycles: A Comparison of Electric Vehicle Battery Degradation. Batteries 5, 42. https://doi.org/10.3390/batteries5020042.

Beaudet, A., Larouche, F., Amouzegar, K., Bouchard, P., Zaghib, K., 2020. Key Challenges and Opportunities for Recycling Electric Vehicle Battery Materials. Sustainability 12, 5837. https://doi.org/10.3390/su12145837.

Ben-Marzouk, M., Pelissier, S., Clerc, G., Sari, A., Venet, P., 2021. Generation of a Real-Life Battery Usage Pattern for Electrical Vehicle Application and Aging Comparison With the WLTC Profile. IEEE Trans. Veh. Technol. 70, 5618–5627. https://doi.org/10.1109/TVT.2021.3077671.

Bibiloni-Mulet, P.A., 2020. Estudi de l'estat de salut de les bateries del vehicle elèctric al final de la seva vida útil. Universitat Politècnica de Catalunya.

BloombergNEF, 2021. Electric Vehicle Outlook 2021.

Canals Casals, L., Amante Garcia, B., Castella Daga, S., 2016a. EL ENVEJECIMIENTO DE LAS BATERÍAS DE UN VEHÍCULO ELÉCTRICO Y CÓMO LO PERCIBE EL CONDUCTOR. DYNA Ing. E Ind. 91, 188–195. https://doi.org/10.6036/7599.

Canals Casals, L., Martinez-Laserna, E., Amante García, B., Nieto, N., 2016b. Sustainability analysis of the electric vehicle use in Europe for CO2 emissions reduction. J. Clean. Prod. 127, 425–437. https://doi.org/10.1016/j.jclepro.2016.03.120.

Canals Casals, L., Rodríguez, M., Corchero, C., Carrillo, R.E., 2019. Evaluation of the End-of-Life of Electric Vehicle Batteries According to the State-of-Health. World Electr. Veh. J. 10, 63. https://doi.org/10.3390/wevj10040063.

Casals, L.C., Etxandi-Santolaya, M., Bibiloni-Mulet, P.A., Corchero, C., Trilla, L., 2022. Electric Vehicle Battery Health Expected at End of Life in the Upcoming Years Based on UK Data 17.

European Commission, 2020. Proposal for a Regulation concerning batteries and waste batteries, repealing Directive 2006/66/EC and amending Regulation (EU) No 2019/1020.

de Hoog, J., Timmermans, J.-M., Ioan-Stroe, D., Swierczynski, M., Jaguemont, J., Goutam, S., Omar, N., Van Mierlo, J., Van Den Bossche, P., 2017. Combined cycling and calendar capacity fade modeling of a Nickel-Manganese-Cobalt Oxide Cell with real-life profile validation. Appl. Energy 200, 47–61. https://doi.org/10.1016/j.apenergy.2017.05.018.

Ellingsen, L.A.-W., Thorne, R.J., Figenbaum, E., n.d. Comparative life cycle assessment of mid-sized electric, diesel, and gasoline passenger vehicles 10.

Etxandi-Santolaya, M., Casals, L., Corchero, C., 2022. Redefining the EV Battery End of Life: Internal Resistance Related Limitations. Bochum, Germany.

Herle, A., Channegowda, J., Prabhu, D., 2021. Overcoming limited battery data challenges: A coupled neural network approach. Int. J. Energy Res. 45, 20474–20482. https://doi.org/10.1002/er.7081.

Hosen, M.S., Kalogiannis, T., Youssef, R., Karimi, D., Behi, H., Jin, L., Van Mierlo, J., Berecibar, M., 2021. Twin-model framework development for a comprehensive battery lifetime prediction validated with a realistic driving profile. Energy Sci. Eng. 9, 2191–2201. https://doi.org/10.1002/ese3.973.

Hu, S., Chen, P., Xin, F., Xie, C., 2019. Exploring the effect of battery capacity on electric vehicle sharing programs using a simulation approach. Transportation Research Part D: Transport and Environment 77, 164–177.

Hua, Y., Liu, X., Zhou, S., Huang, Y., Ling, H., Yang, S., 2021. Toward Sustainable Reuse of Retired Lithium-ion Batteries from Electric Vehicles. Resour. Conserv. Recycl. 168, 105249 https://doi.org/10.1016/j.resconrec.2020.105249.

IEA, 2021. Global EV Outlook 2021 101.

Jaguemont, J., Boulon, L., Dubé, Y., 2016. A comprehensive review of lithium-ion batteries used in hybrid and electric vehicles at cold temperatures. Appl. Energy 164, 99–114. https://doi.org/10.1016/j.apenergy.2015.11.034.

Kotak, Y., Marchante Fernández, C., Canals Casals, L., Kotak, B.S., Koch, D., Geisbauer, C., Trilla, L., Gómez-Núñez, A., Schweiger, H.-G., 2021. End of Electric Vehicle Batteries: Reuse vs. Recycle. Energies 14, 2217. https://doi.org/10.3390/en14082217.

Kurdve, M., Zackrisson, M., Johansson, M.I., Ebin, B., Harlin, U., 2019. Considerations when Modelling EV Battery Circularity Systems. Batteries 5, 40. https://doi.org/10.3390/batteries5020040.

Lawder, M.T., Northrop, P.W.C., Subramanian, V.R., 2014. Model-Based SEI Layer Growth and Capacity Fade Analysis for EV and PHEV Batteries and Drive Cycles. J. Electrochem. Soc. 161, A2099–A2108. https://doi.org/10.1149/2.1161412jes.

Leurent, F., Windisch, E., 2011. Triggering the development of electric mobility: a review of public policies. Eur. Transp. Res. Rev. 3, 221–235. https://doi.org/10.1007/s12544-011-0064-3.

Ma, Y., Houghton, T., Cruden, A., Infield, D., 2012. Modeling the Benefits of Vehicle-to-Grid Technology to a Power System. IEEE Trans. Power Syst. 27, 1012–1020. https://doi.org/10.1109/TPWRS.2011.2178043.
Marmiroli, B., Venditti, M., Dotelli, G., Spessa, E., 2020. The transport of goods in the urban environment: A comparative life cycle assessment of electric, compressed natural gas and diesel light-duty vehicles. Appl. Energy 260, 114236. https://doi.org/10.1016/j.apenergy.2019.114236.
Martinez-Laserna, E., Gandiaga, I., Sarasketa-Zabala, E., Badeda, J., Stroe, D.-I., Swierczynski, M., Goikoetxea, A., 2018. Battery second life: Hype, hope or reality? A critical review of the state of the art. Renew. Sustain. Energy Rev. 93, 701–718. https://doi.org/10.1016/j.rser.2018.04.035.
Milios, L., 2021. Overarching policy framework for product life extension in a circular economy—A bottom-up business perspective. Environ. Policy Gov. 31, 330–346. https://doi.org/10.1002/eet.1927.
Montes, T., Etxandi-Santolaya, M., Eichman, J., Ferreira, V.J., Trilla, L., Corchero, C., 2022. Procedure for Assessing the Suitability of Battery Second Life Applications after EV First Life. Batteries 8, 122. https://doi.org/10.3390/batteries8090122.
Nilsen, H.R., 2019. The hierarchy of resource use for a sustainable circular economy. Int. J. Soc. Econ. 47, 27–40. https://doi.org/10.1108/IJSE-02-2019-0103.
Potting, J., Hanemaaijer, A., Hoekstra, R., Lijzen, J., 2018. Circular economy: what we want to know and can measure 20.
Pyne, M., Yurkovich, B.J., Yurkovich, S., 2019. Generation of Synthetic Battery Data with Capacity Variation. In: 2019 IEEE Conference on Control Technology and Applications (CCTA). IEEE, Hong Kong, China, pp. 476–480. https://doi.org/10.1109/CCTA.2019.8920488.
Quirama, L.F., Giraldo, M., Huertas, J.I., Tibaquirá, J.E., Cordero-Moreno, D., 2021. Main characteristic parameters to describe driving patterns and construct driving cycles. Transp. Res. Part Transp. Environ. 97, 102959 https://doi.org/10.1016/j.trd.2021.102959.
Ravey, A., Watrin, N., Blunier, B., Bouquain, D., Miraoui, A., 2011. Energy-Source-Sizing Methodology for Hybrid Fuel Cell Vehicles Based on Statistical Description of Driving Cycles. IEEE Trans. Veh. Technol. 60, 4164–4174. https://doi.org/10.1109/TVT.2011.2158567.
Richter, J.L., 2022. A circular economy approach is needed for electric vehicles. Nat. Electron. 5, 5–7. https://doi.org/10.1038/s41928-021-00711-9.
Sanguesa, J.A., Torres-Sanz, V., Garrido, P., Martinez, F.J., Marquez-Barja, J.M., 2021. A Review on Electric Vehicles: Technologies and Challenges. Smart Cities 4, 372–404. https://doi.org/10.3390/smartcities4010022.
Saxena, S., Le Floch, C., MacDonald, J., Moura, S., 2015. Quantifying EV battery end-of-life through analysis of travel needs with vehicle powertrain models. J. Power Sources 282, 265–276. https://doi.org/10.1016/j.jpowsour.2015.01.072.
Schäuble, J., Kaschub, T., Ensslen, A., Jochem, P., Fichtner, W., 2017. Generating electric vehicle load profiles from empirical data of three EV fleets in Southwest Germany. J. Clean. Prod. 150, 253–266. https://doi.org/10.1016/j.jclepro.2017.02.150.
Schwarzer, V., Ghorbani, R., 2013. Drive Cycle Generation for Design Optimization of Electric Vehicles. IEEE Trans. Veh. Technol. 62, 89–97. https://doi.org/10.1109/TVT.2012.2219889.
Simon, B., Ziemann, S., Weil, M., 2015. Potential metal requirement of active materials in lithium-ion battery cells of electric vehicles and its impact on reserves: Focus on Europe. Resour. Conserv. Recycl. 104, 300–310. https://doi.org/10.1016/j.resconrec.2015.07.011.
Sommerville, R., Zhu, P., Rajaeifar, M.A., Heidrich, O., Goodship, V., Kendrick, E., 2021. A qualitative assessment of lithium ion battery recycling processes. Resour. Conserv. Recycl. 165, 105219 https://doi.org/10.1016/j.resconrec.2020.105219.
Souffran, G., Miegeville, L., Guerin, P., 2011. Simulation of real-world vehicle missions using a stochastic Markov model for optimal design purposes. In: 2011 IEEE Vehicle Power and Propulsion Conference. IEEE, Chicago, IL, USA, pp. 1–6. https://doi.org/10.1109/VPPC.2011.6043130.
Tazelaar, E., Bruinsma, J., Veenhuizen, B., van den Bosch, P., 2009. Driving cycle characterization and generation, for design and control of fuel cell buses. World Electr. Veh. J. 3, 812–819. https://doi.org/10.3390/wevj3040812.
UK Department for Transport, n.d. Vehicle licensing statistics data files [WWW Document]. GOV.UK. URL https://www.gov.uk/government/statistical-data-sets/vehicle-licensing-statistics-data-files (accessed 7.5.22).
Weil, M., Ziemann, S., Peters, J., 2018. The Issue of Metal Resources in Li-Ion Batteries for Electric Vehicles. In: Pistoia, G., Liaw, B. (Eds.), Behaviour of Lithium-Ion Batteries in Electric Vehicles. Green Energy and Technology. Springer International Publishing, Cham, pp. 59–74. https://doi.org/10.1007/978-3-319-69950-9_3.
Zhao, X., Zhao, X., Yu, Q., Ye, Y., Yu, M., 2020. Development of a representative urban driving cycle construction methodology for electric vehicles: A case study in Xi'an. Transp. Res. Part Transp. Environ. 81, 102279 https://doi.org/10.1016/j.trd.2020.102279.